SUPPORTING INFORMATION

Oxygen-generating Hybrid Polymeric Nanoparticles with Encapsulated Doxorubicin and Chlorin e6 for Trimodal Imaging-Guided Combined Photodynamic-Chemotherapy

DanRong Hu, LiJuan Chen, Ying Qu, JinRong Peng, BingYang Chu, Kun Shi, Ying Hao, Lin Zhong, MengYao Wang, ZhiYong Qian*

State Key Laboratory of Biotherapy and Cancer Center, West China Hospital, West China Medical School, Sichuan University, and Collaborative Innovation Center. Chengdu 610041, PR China

* Corresponding authors. Tel: +86-28-85501986, E-mail address: anderson-qian@163.com (Z.Y. Qian).

Table S1 Properties of PCLA-PEG-PCLA copolymers

Polymer	Theoretical molecular weight ([DLLA]/[CL]/[PEG][a]	Mn/Da (Theoretical)[a]	[LA] /[CL]/[PEG][b]	Mn/Da (^{1}H NMR)[b]
PCLA-PEG-PCLA	14400/21600/4000	40000	13744/20221/4000	37965

[a] Calculated by feed ratio.

[b] Calculated by ^{1}H NMR.

Table S2 Physicochemical characteristics of nanoparticles

DOX loaded samples	DLC[a] (%)			EE[b] (%)			PS[c] (nm)	PDI[d]
	DOX	Ce6	MnO_2	DOX	Ce6	MnO_2		
blank NPs	/	/	/	/	/	/	91.9±2.3	0.181±0.087
DOX NPs	9.9	/	/	87.9	/	/	105.5±0.7	0.126±0.077
Ce6 NPs	/	4.8	/	/	99.6	/	98.5±1.3	0.156±0.034
MnO_2 NPs	/	/	2.0	/	/	74.0	110.4±3.6	0.223±0.053
CD NPs	10.2	4.7	/	90.8	98.7	/	103.5±2.5	0.178±0.039
CM NPs	/	4.8	1.9	/	99.6	70.1	113.6±2.9	0.184±0.062
DM NPs	9.4	/	1.9	83.0	/	70.5	128.4± 2.2	0.194±0.054
CDM NPs	9.5	4.7	1.8	83.8	98.7	66.6	123.6±2.9	0.204±0.049

[a] Drug loading content of DOX (1st line), Ce6 (2nd line) and/or MnO_2 (3rd line).

[b] Encapsulated efficiency of DOX (1st line), Ce6 (2nd line) and/or MnO_2 (3rd line).

[c] Mean diameter of nanoparticles determined by dynamic light scattering.

[d] Polydispersity index (PDI) of nanoparticles size.

Table S3 Pharmacokinetic parameters of free DOX, DOX NPs, CD NPs and CDM NPs in rat after i.v. injection.

Parameters	free DOX	DOX NPs	CD NPs	CDM NPs
C_{max} (μg/mL)	4.0 ± 0.4	69.6±5.4	80.4±3.5	115.6±3.8
$T_{1/2\alpha}$ (h)	0.06±0.01	0.10±0.02	0.12±0.04	0.10±0.02
AUC $_{(0\text{-}t)}$ (μg/mL·h)	7.6±0.7	80.7±3.5	76.4±9.2	102.0±14.5

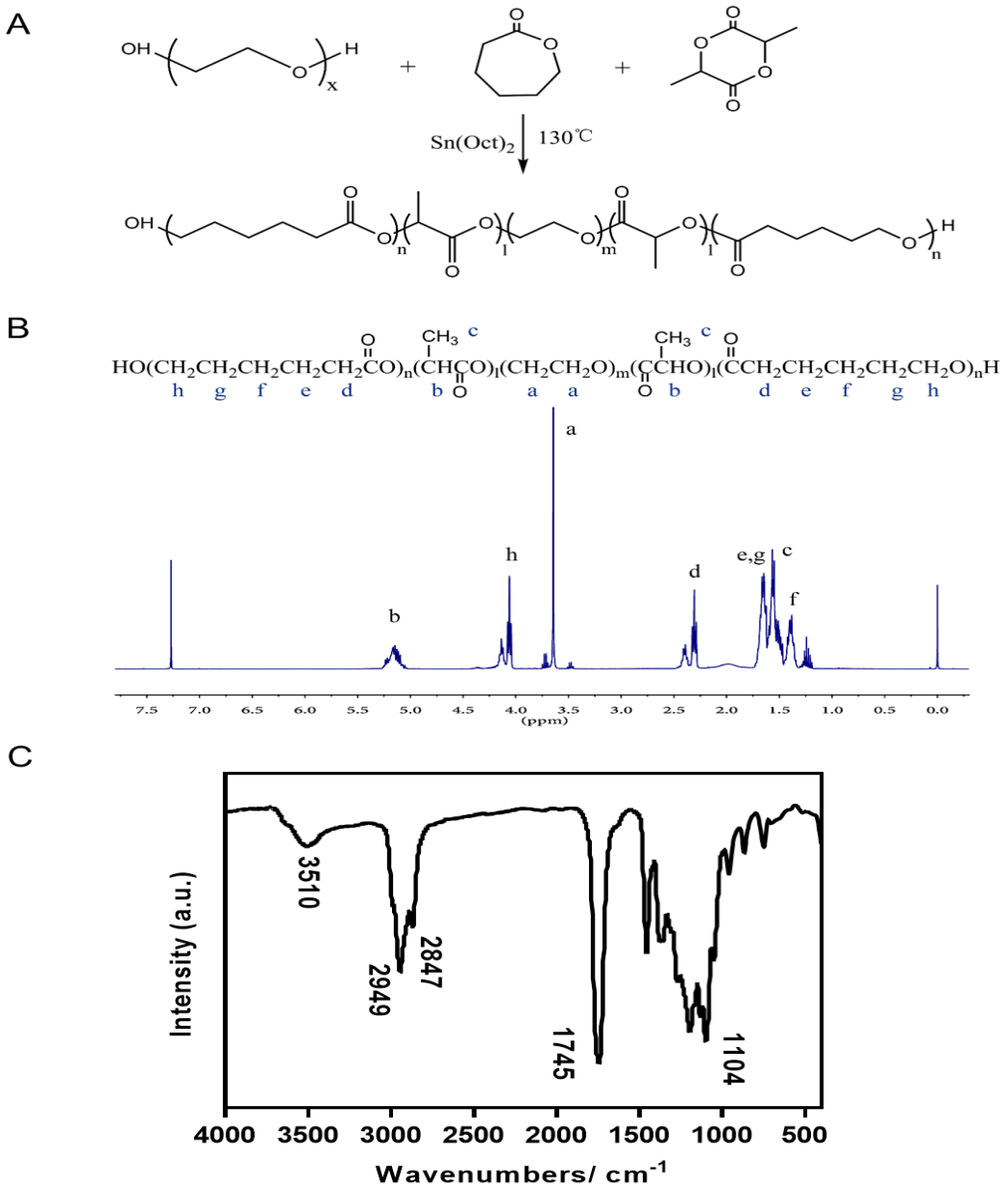

Figure S1 (A) Synthesis scheme of PCLA-PEG-PCLA copolymers. (B) Representative ^{1}H-NMR spectrum (400 MHz) of PCLA-PEG-PCLA copolymer in $CDCl_3$. (C) FT-IR spectrum of PCLA-PEG-PCLA copolymer.

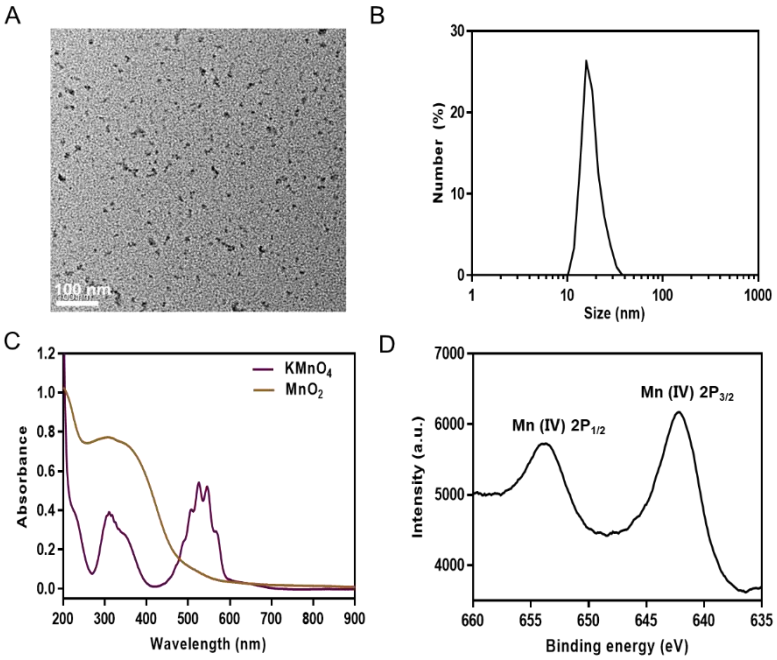

Figure S2 Characterization of colloidal MnO_2. (A) TEM image. Colloidal MnO_2 (~15 nm) were stabilized by positively charged PAH. (B) Size distribution measured by dynamic light scattering (DLS). (C) UV-vis absorption spectra of $KMnO_4$ and colloidal MnO_2. After the reaction with PAH, the $KMnO_4$ peaks (315, 525 and 545 nm) disappeared, and a new broad peak around 300 nm-400nm appeared, an indicator of the formation of colloidal MnO_2. (D) X-ray photoelectron spectroscopy (XPS) spectrum of MnO_2. As is evident, Mn (IV) $2P_{3/2}$ and Mn (IV) $2P_{1/2}$ peak are centered at about 642.3 eV and 653.7 eV, with a spin-energy separation of 11.7 eV, which confirms the formation of Mn (IV)O_2.

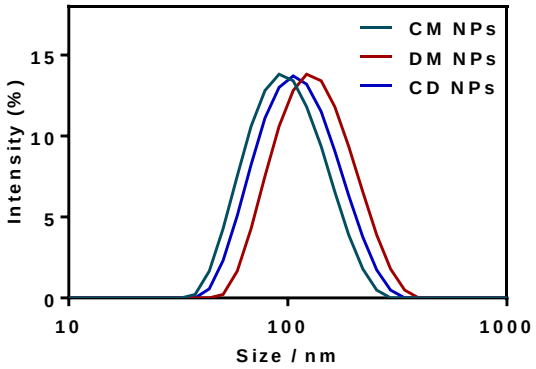

Figure S3 Size distribution of CM NPs, DM NPs and CD NPs measured by dynamic light scattering (DLS).

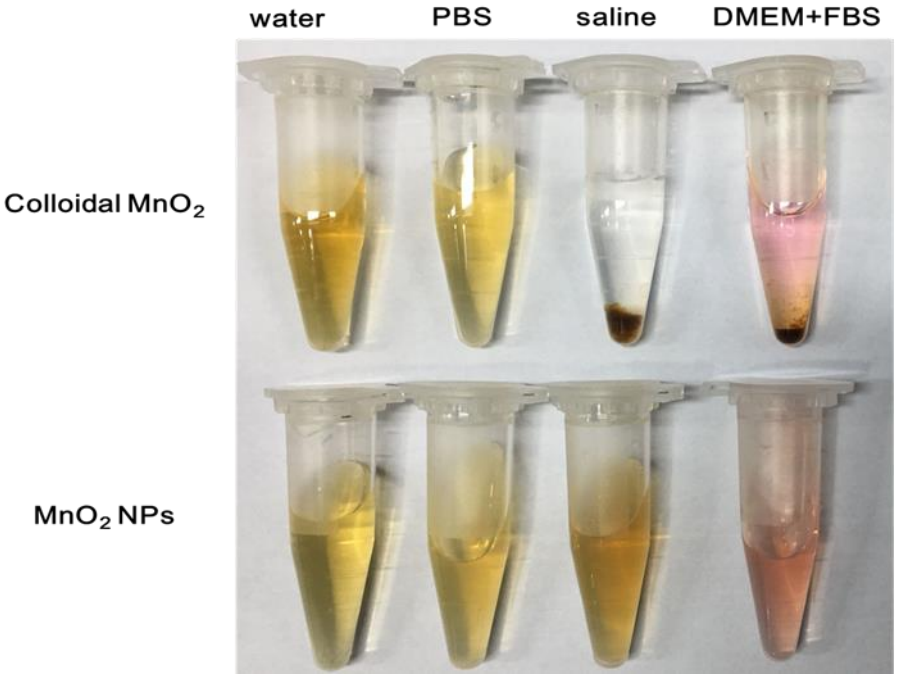

Figure S4 Picture of colloidal MnO_2 and MnO_2 NPs in various aqueous media: water, PBS (pH 7.4, 0.1 M), normal saline (0.9% NaCl) and DMEM cell medium containing 50% fetal bovine serum (FBS). Colloidal MnO_2 undergo aggregation in saline or cell culture medium, while MnO_2 NPs are stable in these media.

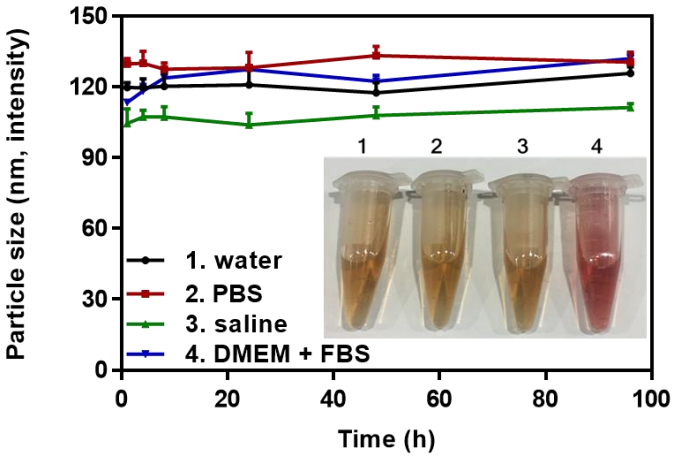

Figure S5 The size stability of CDM NPs in various aqueous media: water, PBS (pH 7.4, 0.1 M), normal saline (0.9% NaCl) and DMEM cell medium containing 50% fetal bovine serum (FBS). The insert shows picture of CDM NPs in various media after 15-days incubation.

A

neutral conditions (pH 7.4):

$$2H_2O_2 \xrightarrow{MnO_2} 2H_2O + O_2\uparrow$$

B

acidic conditions (pH 6.5):

$$MnO_2 + H_2O_2 \longrightarrow Mn^{2+} + 2H_2O + O_2\uparrow$$

$$2MnO_2 + 4H^+ \longrightarrow 2Mn^{2+} + 2H_2O + O_2\uparrow$$

Figure S6 The equations of redox reaction between MnO_2 and H_2O_2 in (A) neutral solutions (pH = 7.4) and (B) acidic solutions (pH = 6.5).

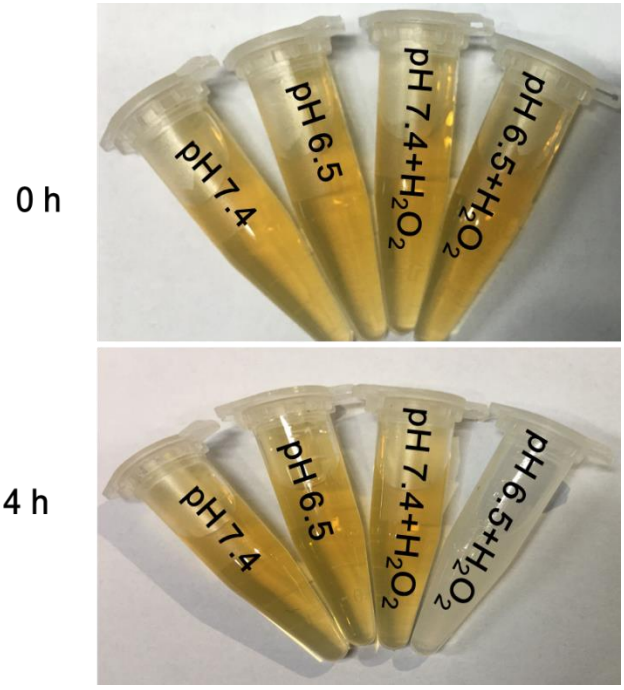

Figure S7 Degradation photos of MnO_2 NPs dispersed in pH 7.4 or pH 6.5 PBS with or without H_2O_2 at 0 h and 4 h. MnO_2 in nanoparticles degraded rapidly under pH 6.5 in the presence of H_2O_2, and almost all MnO_2 converted to colorless Mn^{2+} ions in 4 h. In contrast, MnO_2 appeared to show limited change in other conditions.

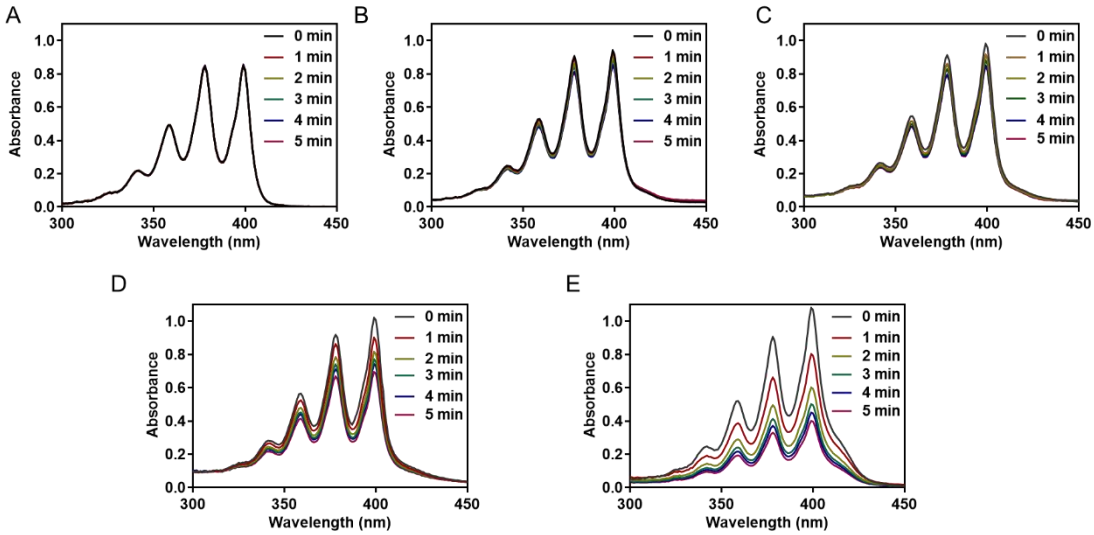

Figure S8 UV-vis absorption spectra of ABDA in different samples at designated time (t = 0-5 min) irradiation of laser (λ = 660 nm) with the power density = 100 mW/cm^2: (A) PBS 6.5; (B) free Ce6 in PBS 6.5; (C) Ce6 NPs in PBS 6.5; (D) CM NPs in PBS 7.4; (E) CM NPs in PBS 6.5. All samples were at the same Ce6 concentration and 30% H_2O_2 solutions were added to maintain the final concentration of H_2O_2 at 100 μM.

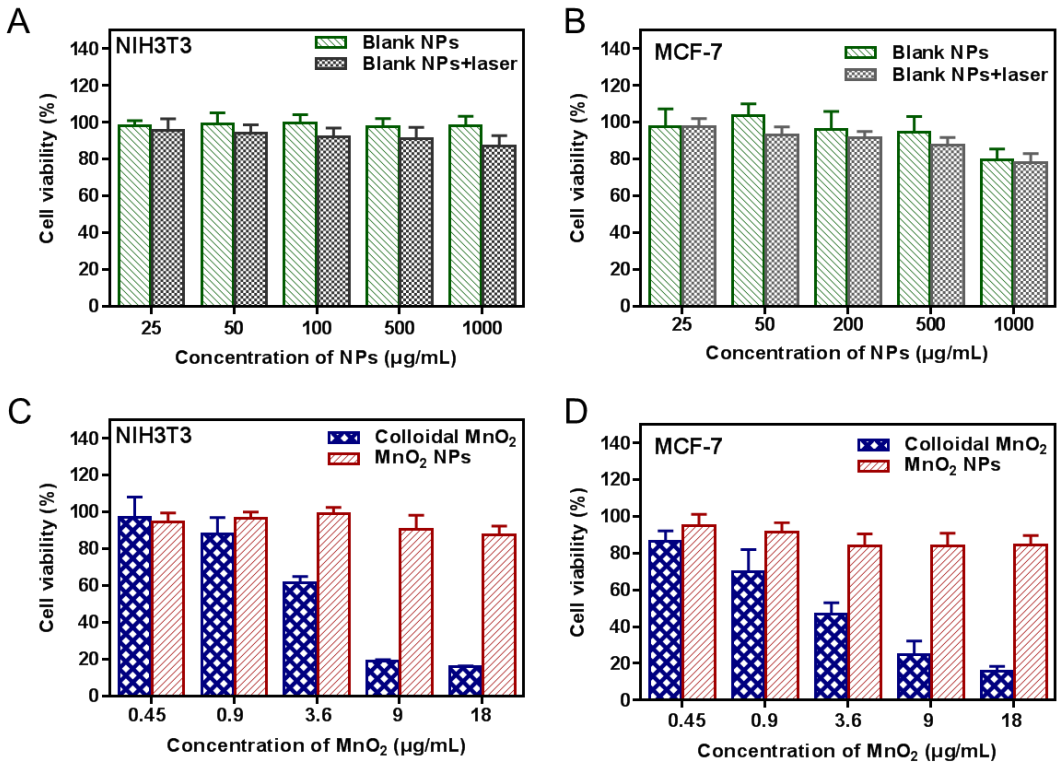

Figure S9 Relative viabilities of NIH 3T3 and MCF-7 cells after incubation with various concentrations of blank NPs, blank NPs with laser irradiation, colloidal MnO_2 and MnO_2 NPs for 24 h.

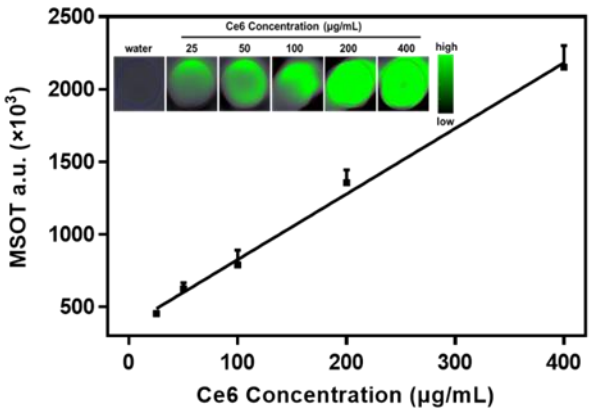

Figure S10 Linear correlation of PA signals of Ce6 in CDM NPs against its corresponding concentrations. Inserted is PA imaging of CDM NPs at indicated Ce6 concentrations (680 nm).

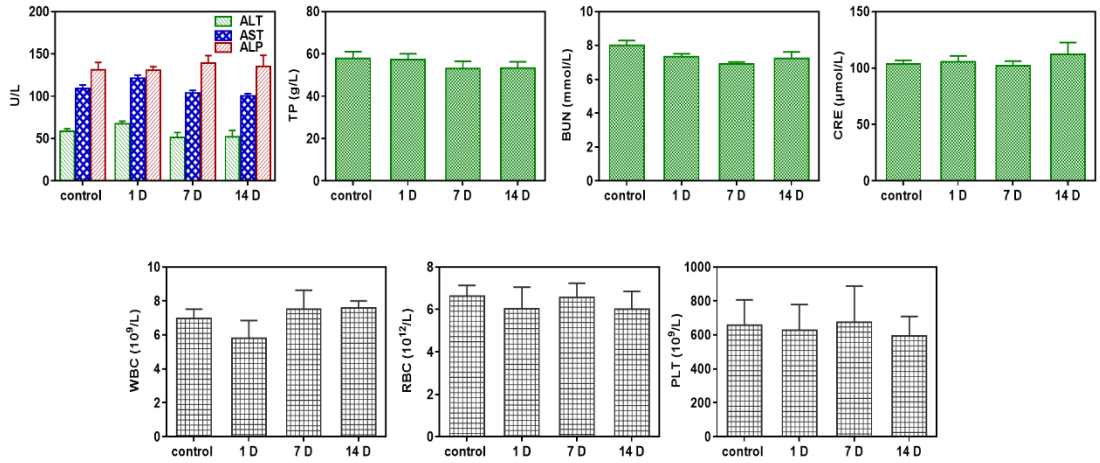

Figure S11 Blood biochemistry and hematology data of female Balb/c mice treated with MnO_2 NPs at the dose of 5 mg/kg at 1, 7, and 14-days post-injection. The examined parameters included alkaline phosphatase (ALP), aminotransferase (ALT), aminotransferase (AST), total protein (TP), blood urea nitrogen (BUN), creatinine (CRE), white blood cell (WBC) counts, red blood cell (RBC) counts and platelets (PLT). All parameters were close to those of the control healthy mice and within the normal reference ranges. Statistics are based on three mice per data point.

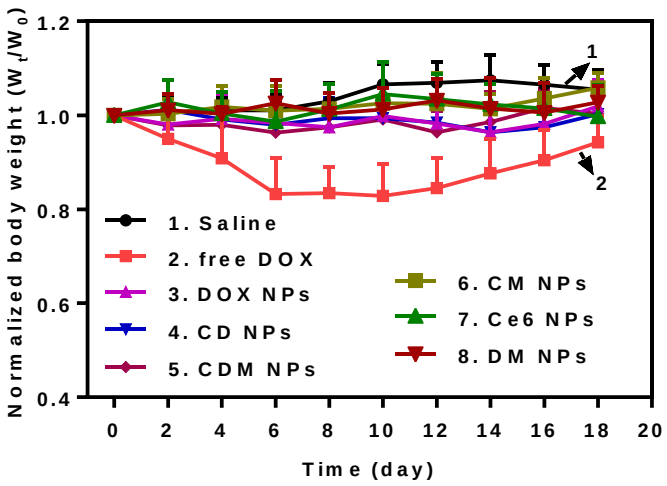

Figure S12 Normalized body weight of mice bearing MCF-7 tumors after various treatments as indicated. Error bars represent SD (n = 5).

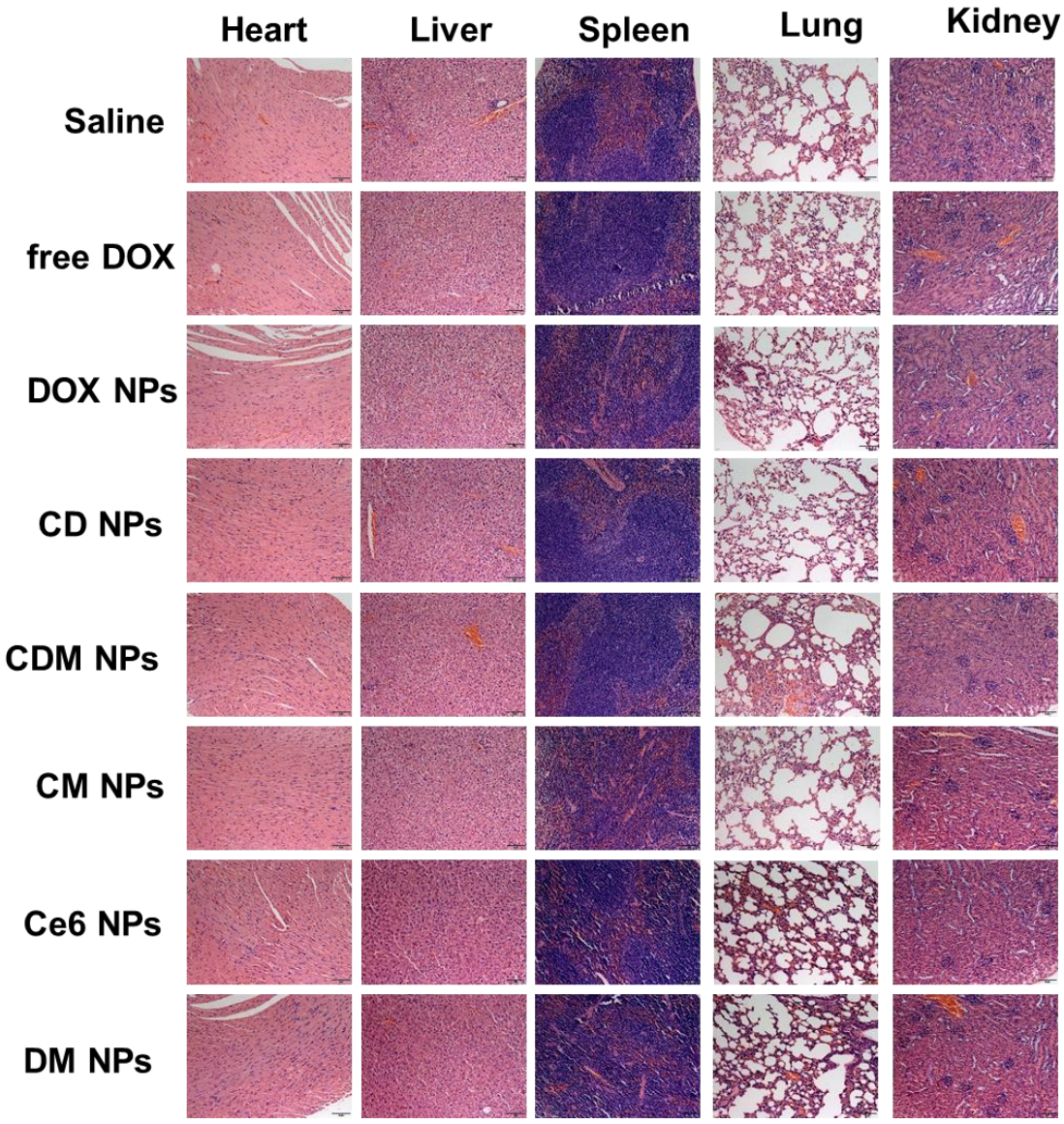

Figure S13 Representative H&E stained images of major organs including heart, liver, spleen, lung and kidney collected from the untreated mice and mice treated with various formulations at 18-days post-injection. Images were acquired at 200 × magnification. No obvious organ damage or lesion was observed for CDM NPs treated mice.